

# Inclusion in Microporous $\beta$ -Bis(1,1,1-trifluoro-5,5-dimethyl-5-methoxyacetylacetonato)copper(II), an Organic Zeolite Mimic<sup>†</sup>

Dmitriy V. Soldatov<sup>‡</sup> and John A. Ripmeester\*

Steacie Institute for Molecular Sciences, National Research Council of Canada,  
Ottawa K1A 0R6, Canada

Received December 6, 1999. Revised Manuscript Received February 24, 2000

In this contribution, we show that the porous  $\beta$ -form of the title complex preserves its host lattice pore structure in the presence of more than 100 guests. Among the species that are able to promote the  $\alpha$ -to- $\beta$  transformation and that are capable of being included as guests are the gaseous and condensed hydrocarbons, their halo derivatives, alcohols, diols, aldehydes, ketones, ethers, esters, ethers of inorganic acids, acids, nitriles, and a variety of substituted aromatics. The empty  $\beta$ -form behaves like a microporous sponge, instantly absorbing significant quantities even of highly volatile compounds such as methane, ethane, and propane. The material demonstrates zeolite-like behavior, not only from the robustness of the empty pore structure, but also from its propensity for efficient adsorption and desorption. The thermal stability of inclusions with normal paraffins increases from 142 °C (incongruent melting) to 163.5 °C (true melting) in the series from *n*-C5 to *n*-C16, while the guest-free  $\alpha$ -form of the complex melts at 157 °C. The interaction of the complex with alcohols illustrates competing options between chemical bonding to copper and physical sorption into the microporous  $\beta$ -form. Methanol and ethanol coordinate to copper, thereby taking part in building, respectively, 2-D and 1-D polymers, whereas higher alcohols induce conversion to a 3-D  $\beta$ -form, stabilizing this porous modification by inclusion. From the observed stoichiometry and thermal stability, the host matrix is shown to be capable of molecular recognition of alcohols that have a shape and dimensions complementary to available pore geometry. Finally, the prospects for the rational design of new 3-D microporous polymers of bis-chelate building blocks are discussed.

## Introduction

Of the numerous known supramolecular architectures only a few are known to remain intact upon variation of one or more of its components. Recently, much effort has been invested in the design and study of new microporous solids capable of including a wide range of guests, meanwhile preserving the overall structure of the product. In such cases the detailed features of each architectural type may be employed to illustrate selectivity. This arises from the characteristic inclusion properties of the host voids related to shape and size, the restricted orientation of included species, the specific location of guest sites inside the parent matrix, etc. Metal complexes are very useful for such design, because the information borne by easily modified building units tends to be superimposed on the basic architecture by means of readily induced self-assembly. In other words, programming of the selective functions is possible by delicate control of the matrix. One of the first

such attempts reported in the literature inspired a certain optimism, as structural studies of more than 300 tetraarylporphyrin-based clathrates revealed a remarkable preservation of the host structure.<sup>1</sup> These solids were referred to as “microporous sponges” because the channel characteristic of this lattice can accommodate a wide range of ligands and solvent “guest” molecules. Also, tetrapyrroline Werner hosts in several dozens of inclusions preserve their principal architecture even with widely varying constituents.<sup>2</sup> Among the two- and three-dimensional metal–complex hosts, polymeric cyanometalates are known to keep their main structural motif and their ability to tolerate extremely wide host

(1) (a) Li, H.; Eddaoudi, M.; O’Keeffe, M.; Yaghi, O. M. *Nature* **1999**, *402*, 276–279. (b) Byrn, M. P.; Curtis, C. J.; Hsiou, Y.; Khan, S. I.; Sawin, P. A.; Terzis, A.; Strouse, C. E. In *Comprehensive Supramolecular Chemistry*; MacNicol, D. D., Toda, F., Bishop, R., Eds.; Pergamon: Oxford, 1996; Vol. 6, pp 715–732. (c) Byrn, M. P.; Curtis, C. J.; Hsiou, Y.; Khan, S. I.; Sawin, P. A.; Tendick, S. K.; Terzis, A.; Strouse, C. E. *J. Am. Chem. Soc.* **1993**, *115*, 9480–9497. (d) Byrn, M. P.; Curtis, C. J.; Goldberg, I.; Huang, T.; Hsiou, Y.; Khan, S. I.; Sawin, P. A.; Tendick, S. K.; Terzis, A.; Strouse, C. E. *Mol. Cryst. Liq. Cryst.* **1992**, *211*, 135–140. (e) Byrn, M. P.; Curtis, C. J.; Goldberg, I.; Hsiou, Y.; Khan, S. I.; Sawin, P. A.; Tendick, S. K.; Strouse, C. E. *J. Am. Chem. Soc.* **1991**, *113*, 6549–6557. (f) Byrn, M. P.; Strouse, C. E. *J. Am. Chem. Soc.* **1991**, *113*, 2501–2508. (g) Byrn, M. P.; Curtis, C. J.; Khan, S. I.; Sawin, P. A.; Tsurumi, R.; Strouse, C. E. *J. Am. Chem. Soc.* **1990**, *112*, 1865–1874.

<sup>†</sup> Issued as NRCC No. 43835.

\* Corresponding author: Steacie Institute for Molecular Sciences, National Research Council of Canada, Ottawa, Ontario, Canada K1A 0R6. E-mail: jar@ned1.sims.nrc.ca. Fax: (613) 998-7833.

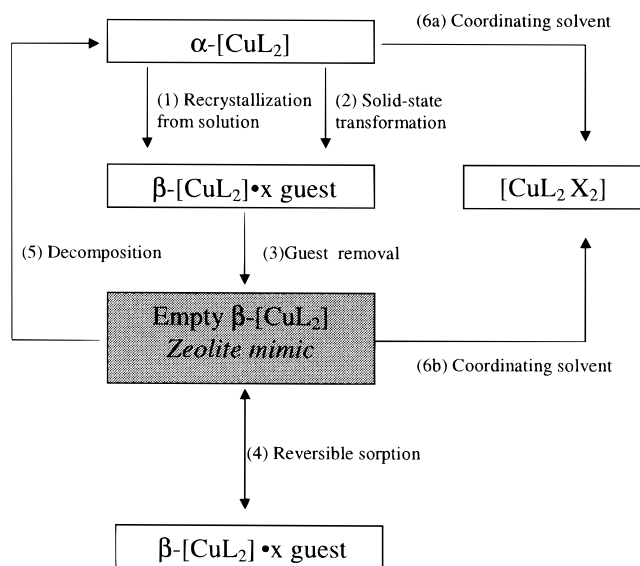
<sup>‡</sup> Permanent Address: Institute of Inorganic Chemistry, Siberian Branch of the Russian Academy of Sciences, Novosibirsk 630090, Russia.

and guest modifications.<sup>3</sup> More recent findings involve cadmium cyanide 3-D networks<sup>4</sup> and coordination frameworks built up out of suitable metal centers and bidentate ligands acting as simple linear spacers.<sup>5</sup>

In exceptional cases the pore structure is preserved so that the structure remains stable kinetically even after significant or complete removal of the included guest. This phenomenon, observed for both metal-organic and organic systems, has evoked considerable interest in recent years and precipitated many attempts to design new microporous materials capable of including organics, thus mimicking important classes of inorganic sorbents such as zeolites. Ideally, such materials should combine, on one hand, the remarkable capacity and selectivity inherent to clathrates and, on the other hand, the speed of sorption and reversibility characteristic of zeolites. Despite much effort, only a few hosts containing organics that form stable porous matrices have been reported so far, and very few of them have been studied in detail. In the literature they are referred to as "organic zeolite analogs" or "organic zeolites".<sup>5</sup>

Recently<sup>6</sup> we reported the synthesis, structural features and main properties of the title host complex  $[\text{CuL}_2]$  ( $\text{L} = \text{L}^- = \text{CF}_3\text{COCHCOC}(\text{OMe})\text{Me}_2$ ). It was found that the complex exists in two polymorphic modifications. The orthorhombic  $\alpha$ -form is stable but has no pores of molecular size or sorption capacity. The trigonal  $\beta$ -form, formed (see Scheme 1) either by recrystallization of the title compound from a suitable solvent

Scheme 1



or by contacting the  $\alpha$ -form with a characteristic transforming compound such as methyl bromide that "switches on" the zeolitic function (see Scheme 1), has channels  $\sim 6 \text{ \AA}$  in diameter. Similar to other zeolite mimics, upon complete removal of the guest, the empty  $\beta$ -form is stable kinetically and retains its porosity as attested by results obtained by two independent methods. Powder diffraction showed the guest-free form to be isostructural with the inclusion compounds, and helium pycnometry showed that 17% of the crystal volume was accessible to helium gas.

In this work, we further illustrate zeolite-like behavior of  $\beta$ - $[\text{CuL}_2]$  by reversibly including gaseous organic species without collapsing the framework into the dense  $\alpha$ -form (Scheme 1). The data obtained previously revealed the great sorption potential of this material and also led to the supposition of very distinct types of behavior for different guests. We elucidate these features by a systematic variation of guest geometry and functional groups. This study also delimits the range of species the title material is capable of absorbing, and identifies strongly coordinating molecules that have the capacity to "switch off" the zeolitic function.

## Results and Discussion

**Inclusion of *n*-Paraffins and Pentanes.** Methane, ethane, and propane do not react with the  $[\text{CuL}_2]$  complex in its stable  $\alpha$ -form under ambient conditions (room temperature and atmospheric pressure) but are readily sorbed into the  $\beta$ -form, as soon as the empty framework is placed in an atmosphere of the respective gas (Scheme 1, reaction 4). *n*-Butane does react with  $\alpha$ - $[\text{CuL}_2]$  as witnessed by the significant increase in sample mass and the complete phase transformation to the  $\beta$ -modification. The dynamics of the weight increase and rate of  $\alpha$ -to- $\beta$  conversion during the reaction indicate that the formation of the  $\beta$ -form is followed immediately by the filling of the pore space (Scheme 1, reaction 2). In contrast, the reverse reaction, that is, clathrate decomposition (in flowing nitrogen) was much slower and more complicated, it probably being the sum of two processes (Scheme 1, reactions 4 and 5). First,

(2) (a) Soldatov, D. V.; Ripmeester, J. A. *Supramol. Chem.* **1998**, *9*, 175–181. (b) Soldatov, D. V.; Lipkowski, J. *J. Inclusion Phenom.* **1998**, *30*, 99–109. (c) Soldatov, D. V.; Dyadin, Yu. A.; Lipkowski, J.; Suwinska, K. *Mendeleev Commun.* **1997**, 100–102. (d) Soldatov, D. V.; Dyadin, Yu. A.; Lipkowski, J.; Ogienko, A. G. *Mendeleev Commun.* **1997**, 11–13. (e) Soldatov, D. V. *J. Inclusion Phenom.* **1995**, *20*, 191–192. (f) Soldatov, D. V.; Lipkowski, J. *J. Struct. Chem.* **1995**, *36*, 979–982.

(3) (a) Iwamoto, T. In *Comprehensive Supramolecular Chemistry*; MacNicol, D. D., Toda, F., Bishop, R., Eds.; Pergamon: Oxford, 1996; Vol. 6, pp 643–690. (b) Iwamoto, T. *J. Inclusion Phenom.* **1996**, *24*, 61–132. (c) Yuge, H.; Noda, Y.; Iwamoto, T. *Inorg. Chem.* **1996**, *35*, 1842–1848. (d) Iwamoto, T. In *Inclusion Compounds*; Atwood, J. L., Davies, J. E. D., MacNicol, D. D., Eds.; Academic Press: London, 1984; Vol. 1, pp 29–57. (e) Iwamoto, T. *J. Mol. Struct.* **1981**, *75*, 51–65. (f) Iwamoto, T. *Israel J. Chem.* **1979**, *18*, 240–245.

(4) (a) Iwamoto, T.; Nishikiori, S.; Kitazawa, T.; Yuge, H. *J. Chem. Soc., Dalton Trans.* **1997**, 4127–4136. (b) Kim, C.; Nishikiori, S.; Iwamoto, T. *Mol. Cryst. Liq. Cryst.* **1996**, *276*, 13–18. (c) Kitazawa, T.; Kikuyama, T.; Takeda, M.; Iwamoto, T. *J. Chem. Soc., Dalton Trans.* **1995**, 3715–3720. (d) Kitazawa, T.; Nishikiori, S.; Iwamoto, T. *J. Chem. Soc., Dalton Trans.* **1994**, 3695–3710. (e) Kitazawa, T.; Nishikiori, S.; Kuroda, R.; Iwamoto, T. *J. Chem. Soc., Dalton Trans.* **1994**, 1029–1037.

(5) (a) Sawaki, T.; Aoyama, Y. *J. Am. Chem. Soc.* **1999**, *121*, 4793–4798. (b) Kepert, C. J.; Rosseinsky, M. J. *Chem. Commun.* **1999**, 375–376. (c) Russel, V. A.; Evans, C. C.; Li, W.; Ward, M. D. *Science* **1997**, *276*, 575. (d) Brunet, P.; Simard, M.; Wuest, J. D. *J. Am. Chem. Soc.* **1997**, *119*, 2737–2738. (e) Kondo, M.; Yoshitomi, T.; Seki, K.; Matsuzaka, H.; Kitagawa, S. *Angew. Chem., Int. Ed. Engl.* **1997**, *36*, 1725. (f) In *Comprehensive Supramolecular Chemistry*; MacNicol, D. D., Toda, F., Bishop, R., Eds.; Pergamon: Oxford, 1996; Vol. 6: see Mak, T. S. W.; Bracke, B. R. F., p 39; Gdanec, M.; Ibragimov, B. T.; Talipov, S. A., pp 139–140; Lipkowski, J., pp 697–698. (g) Yaghi, O. M.; Li, G.; Li, H. *Nature* **1995**, *378*, 703. (h) Venkataraman, D.; Gardner, G. B.; Lee, S.; Moore, J. S. *J. Am. Chem. Soc.* **1995**, *117*, 11600–11601. (i) Ung, A. T.; Gizachew, D.; Bishop, R.; Scudder, M. L.; Dance, I. G.; Craig, D. C. *J. Am. Chem. Soc.* **1995**, *117*, 8745–8756. (g) Ibragimov, B. T.; Talipov, S. A.; Aripov, T. F. *J. Inclusion Phenom.* **1994**, *17*, 317–324. (k) Allison, S. A.; Barrer, R. M. *J. Chem. Soc. A* **1969**, 1717–1723.

(6) Soldatov, D. V.; Ripmeester, J. A.; Shergina, S. I.; Sokolov, I. E.; Zanina, A. S.; Gromilov, S. A.; Dyadin, Yu. A. *J. Am. Chem. Soc.* **1999**, *121*, 4179–4188. For first communication on the title host, see: Gromilov, S. A.; Baydina, I. A.; Zharkova, G. I. *J. Struct. Chem.* **1997**, *38*, 792–798; in Russian version 946–953.

**Table 1. Compositions and Thermal Stability of [CuL<sub>2</sub>]<sup>x</sup>(Paraffin) Inclusions**

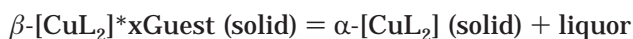
paraffin	quantity of sorbed paraffin			method <sup>a</sup>	melting parameters <sup>b</sup>	
	mass %	mol. (x)	exp. t, °C		t, °C	type
C1	0.9(1)	0.27(3)	20	A		
C2	2.7(1)	0.44(2)	20	A		
C3	5.1(2)	0.56(2)	20	A		
n-C4	7.37(7)	0.616(6)	20	B		
n-C5	6.6(1)	0.442(8)	20	C	142	incongruent
iso-C5	7.5(1)	0.506(7)	20	B	144	incongruent
neo-C5	7.7(1)	0.519(9)	20	B		
n-C6	6.61(7)	0.373(4)	20	C	147	congruent
n-C7	7.05(6)	0.342(3)	20	C	150.5	congruent
n-C8	7.29(5)	0.310(2)	20	C	151	congruent
n-C9	7.30(5)	0.277(2)	20	C	152	congruent
n-C10	7.49(5)	0.256(2)	20	C	154	congruent
n-C11	7.49(4)	0.233(1)	20	C	157	congruent
n-C12	7.79(3)	0.222(1)	20	C	158	congruent
n-C13	7.77(4)	0.205(1)	50	C	159.5	congruent
n-C14	7.40(4)	0.181(1)	90	C	161	congruent
n-C15	7.34(5)	0.168(1)	90	C	161.5	congruent
n-C16	7.35(7)	0.158(1)	90	C	163.5	congruent

<sup>a</sup> See Experimental Section for description. <sup>b</sup> Pure [CuL<sub>2</sub>] host in its  $\alpha$ -form melts congruently at 157 °C.

removal of the guest with the host matrix remaining intact (Scheme 1, reaction 4) demonstrates zeolite-like behavior of the system. The rate of the process is a function of guest content, the first portions of guest butane escaping very quickly (for 100%  $\beta$ -phase, 20% was lost in the first few minutes), and as the reaction progressed, it became increasingly slow. The secondary reaction (Scheme 1, reaction 5) was very slow and seemed independent of guest content. Our experiences indicate that phase conversion is likely to depend on impurities in the material or in the atmosphere (including humidity), the presence of traces of higher hydrocarbons, etc. We limit ourselves to the above notes, as a full elucidation of the phase interconversion kinetics requires further specialized studies.

Pentanes and higher paraffins readily react with  $\alpha$ -[CuL<sub>2</sub>], transforming it into the  $\beta$ -form and filling the available pore volume (Scheme 1, reaction 2). Data on the composition of inclusions with paraffins are listed in Table 1. The quantity of included paraffin increases on going from methane to *n*-butane. For guests larger than *n*-pentane, the included guest mass changes little, as the guest mole ratio decreases steadily with increasing guest size. As for the pentanes, branched species are included in greater quantity as the available pore space is used more effectively.

The stability of the inclusions increases monotonically with the size of the paraffin molecule. Inclusions with pentanes are moderately stable in air and in a sealed tube they melt at 142–144 °C with formation of green liquor and the solid  $\alpha$ -form:



Starting from *n*-hexane, the resulting inclusions undergo true melting, with inclusions of C12 and higher paraffins being thermally more stable than pure host complex.

The increasing stability with increasing paraffin length is a well-known fact for other clathrate systems, especially for inclusions of urea and thiourea.<sup>7</sup> The greater the size of the paraffin, the smaller the ratio of

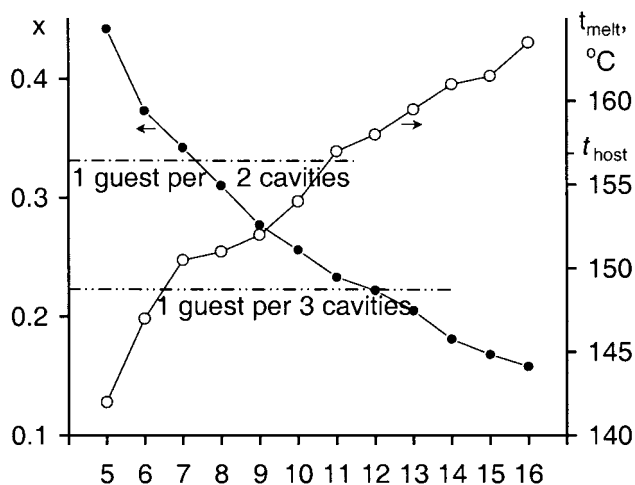


**Figure 1.** Guest–host mole ratios  $x$  (solid circles, left axis) and melting temperatures (open circles, right axis) versus the number of skeletal carbons  $y$  for the guests in  $\beta$ -[CuL<sub>2</sub>]<sup>x</sup>(*n*-C<sub>y</sub>H<sub>2y+2</sub>) inclusions.

intermolecular contacts to covalent bonds for the guest subsystem, and the larger the number of van der Waals contacts between the host and the guest molecules. For urea inclusions the formal dependence of the heats of formation<sup>7,8</sup> and the decomposition temperatures<sup>8</sup> on paraffin size have been obtained, thus allowing a high degree of predictability.

The dependence shown in Figure 1 is more informative when the structure of the title host matrix is taken into account. Unlike that in urea, the channel in  $\beta$ -[CuL<sub>2</sub>] has a variable diameter. When each wide channel portion is filled with one guest molecule, the guest-to-host mole ratio equals  $2/3$ , this actually being observed for a number of aromatic guests,<sup>6</sup> and in the series studied, the inclusion with *n*-butane has a value near to this (Table 1). Larger species should fill two adjacent cavities to give a mole ratio of  $1/3$ , or three adjacent cavities to give a value of  $2/9$ . Comparing compositions and melting temperatures of the compounds (Figure 1), one notices that the guest-to-host mole ratios corresponding to stoichiometric filling of available cavities increases the thermal stability of resulting inclusions. This fact is better illustrated for inclusions with alcohols (see below).

Single-crystal X-ray experiments on the *n*-hexane inclusion reveal that the host structure keeps the structural motif observed previously for the benzene compound.<sup>6</sup> The host molecule (Figure 2, top) is centrosymmetric, thus being *trans*-configured with respect to the ligand substituents. The copper atom is in the square-planar environment of two pairs of chelating oxygens from ligand moieties at distances of 1.92–1.93 Å. Donor oxygens associated with the methoxy groups take part in the formation of two additional interactions each (Table 2): the first is an intramolecular hydrogen

(7) (a) Takemoto, K.; Sonoda, N. In *Inclusion Compounds*; Atwood, J. L., Davies, J. E. D., MacNicol, D. D., Eds.; Academic Press: London, 1984; Vol. 2, pp 47–67. (b) Zimmerschied, W. J.; Dinerstein, R. A.; Weitkamp, A. W.; Marschuer, R. F. *Ind. Eng. Chem.* **1950**, *42*, 1300–1306. (c) Schlenk, W. *Justus Liebigs Ann. Chem.* **1949**, *565*, 204–240 (in German); *Chem. Abstr.* **1950**, *44*, 3900a.

(8) Chekhova, G. N.; Dyadin, Yu. A. *Isv. Sib. Otd. Akad. Nauk SSSR, Ser. Khim. Nauk* **1986**, (No. 2), 66–72 (in Russian); *Chem. Abstr.* **1986**, *105*, 42257f.



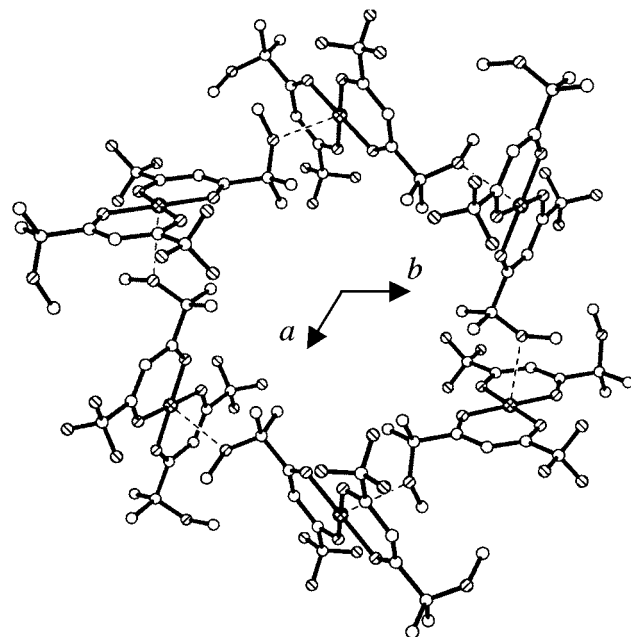
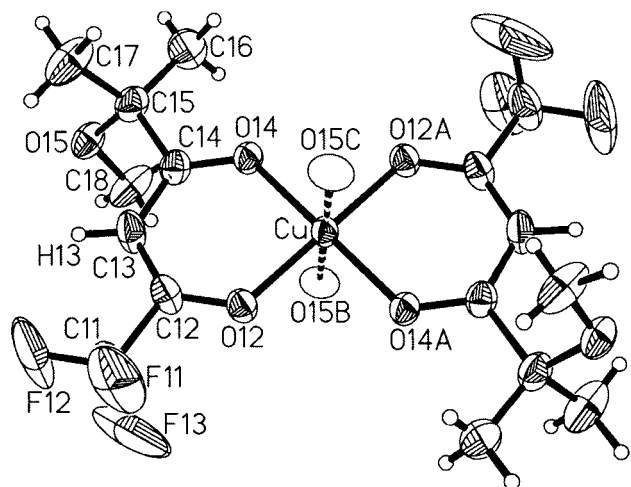


**Figure 2.** Top: Host molecule and oxygen atoms of neighboring hosts in  $\beta$ -[CuL<sub>2</sub>] $\cdot$ 0.38(*n*-hexane). A-labeled atoms are generated by centrosymmetry, O15B and O15C from O15 with ( $\frac{4}{3} - x + y, \frac{2}{3} - x, -\frac{1}{3} + z$ ) and ( $-\frac{1}{3} + x - y, -\frac{2}{3} + x, \frac{4}{3} - z$ ) operators, respectively. Selected bond distances (Å) and angles (deg): Cu–O12, 1.916(1); Cu–O14, 1.932(1); Cu–O15B, 2.709(1); O12–Cu–O14, 92.57(5); O12–Cu–O14A, 87.43(5); O12–Cu–O15B, 92.94(5); O14–Cu–O15B, 82.55(5). Bottom: 3-D host molecular assembly that forms the channel. The six molecules shown are connected to each other and surround the channel, three on a higher and three on a lower level. On different levels, the inner surface of the channel is formed either by methyl or fluoromethyl groups. H-atoms are omitted.

bond to >C–H of the chelate ring, and this interaction must play an important role in fixing the molecule in a definite conformation. The second is the additional intermolecular coordination to the apical coordination sites on copper atoms of the adjacent molecules at 2.71 Å. The latter creates polymer-like 3-D structures possessing channel-shaped voids.

The profile of the channel, obtained as the diameter of the inscribed sphere along the channel axis,<sup>6</sup> is shown in Figure 3, top. The channel stretches along the 3-fold inversion axis, which is the principal axis in the  $R\bar{3}$  space group. The channel capacity may be represented as a 1-D sequence of two inequivalent sorption sites,

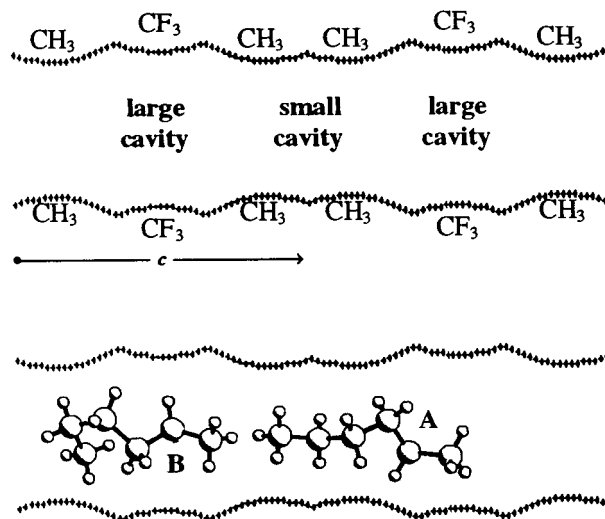


**Figure 3.** Top: Profile of the channel in  $\beta$ -[CuL<sub>2</sub>] $\cdot$ 0.38(*n*-hexane) represented as the diameter of the inscribed sphere along the channel axis (which coincides with the *c*-axis). The locations of the methyl and fluoromethyl groups facing the channel and both large and small cavities are indicated. Bottom: Location of the two guest orientations (all symmetrical or translational equivalencies are omitted): 0.199(7) mole of guest is A-oriented, and 0.181(7) mole is B-oriented.

and for convenience we refer to these as cavities.<sup>9</sup> Small cavities, located about the Wyckoff special position *a* with  $\bar{3}$  point symmetry alternate with large cavities located about the Wyckoff position *b* with the same point symmetry. The difference between these lies not only in the size and shape of the cavity, but also in the nature of the cavity walls: the small cavity is formed from host methyl groups, whereas the trifluoromethyl groups take part in constructing the walls of the large cavity. Large thermal ellipsoids (see Figure 2, top) and disorder of the trifluoromethyl groups are consistent with a bending of the latter into the inner channel space and the friability of the channel walls near the widest part of the channel.

The hexane guest molecules are badly disordered in the channels. As well as the inevitable disorder about the 3-fold inversion axis, a number of symmetrically inequivalent orientations are expected. We attempted to find these by superimposing dozens of conformations onto the residual electron density centers after the host structure was determined. Upon successive refinements within this model, orientations having low occupancy factors were removed, thus leading us to a final solution with only two symmetrically inequivalent orientations. Surprisingly, with these two, having 0.199(7) and 0.181(7) guest-to-host mole ratios, the *R* value dropped to 0.037 for quite reasonable guest arrangements along the channel (Figure 3). The molecule in the first orientation has its greater part positioned tightly inside the small cavity, whereas the remaining part looks into the large cavity, bending close to the cavity wall. The molecule in the second orientation is located mainly in the large cavity, inserting an open-ring-shaped portion into the

(9) An analogous description was used before to describe the 3-D pore space in the first "organic zeolite"  $\beta$ -IM(4-methylpyridine)<sub>4</sub>(NCS)<sub>2</sub>.<sup>10</sup> For that structure, different modes and occupancies of two types of sorption centers were observed that depended on the parameters of the guest component and its concentration (pressure) over the host matrix.<sup>11</sup>

**Table 2. Lengths (Å) and Angles (deg) of Additional Bonds within and among Coordination Units<sup>a</sup>**

compound, framework topology	bond type	atom D	atom A	D...A	atom H	D...H	D...H-A
$\beta$ -[CuL <sub>2</sub> ] $\cdot$ 0.38 ( <i>n</i> -hexane), 3-D polymer	coordination	O15B	Cu	2.709(1)			
	<b>intermolecular</b> coordination	O15C	Cu	2.709(1)			
	<b>intermolecular</b> hydrogen <b>intramolecular</b> coordination	O15	C13	2.907(2)	H13	2.68(3)	95(2)
$\beta$ -[CuL <sub>2</sub> ] $\cdot$ <sup>2</sup> / <sub>3</sub> ( <i>tert</i> -butanol), 3-D polymer	<b>intermolecular</b> coordination	O15B	Cu	2.738(2)			
	<b>intermolecular</b> coordination	O15C	Cu	2.738(2)			
	<b>intermolecular</b> hydrogen <b>intramolecular</b> coordination	O15	C13	2.894(4)	H13	2.64(4)	99(3)
	<b>intermolecular</b> coordination	O15'B	Cu	2.85(2)			
	<b>intermolecular</b> coordination	O15'C	Cu	2.85(2)			
	<b>intermolecular</b> hydrogen <b>intramolecular</b> coordination	O15'	C13	2.80(2)	H13	2.50(4)	101(3)
	<b>intermolecular</b> hydrogen	O15	C13	2.798(2)	H13	2.51(2)	99(2)
[Cu(MeOH) <sub>2</sub> L <sub>2</sub> ], 2-D polymer	<b>intermolecular</b> hydrogen	O15	O1D	2.889(2)	H1D	2.16(3)	173(3)
{[Cu(EtOH)L <sub>2</sub> ] <sub>2</sub> [CuL <sub>2</sub> ]}, 1-D polymer	<b>intermolecular</b> coordination	O35E	Cu1	2.888(1)			
	<b>intermolecular</b> hydrogen	O15	C13	2.829(3)	H13	2.48(2)	103(2)
	<b>intramolecular</b> hydrogen	O25	C23	2.855(2)	H23	2.55(2)	101(2)
	<b>intermolecular</b> hydrogen	O35	C33	2.910(2)	H33	2.70(2)	95(2)
	<b>intramolecular</b>						

<sup>a</sup> Labeled atoms are generated by the follows symmetry operators: B = (<sup>1</sup>/<sub>3</sub> - x + y, <sup>2</sup>/<sub>3</sub> - x, -<sup>1</sup>/<sub>3</sub> + z); C = (-<sup>1</sup>/<sub>3</sub> + x - y, -<sup>2</sup>/<sub>3</sub> + x, <sup>4</sup>/<sub>3</sub> - z); D = (x, <sup>1</sup>/<sub>2</sub> - y, -<sup>1</sup>/<sub>2</sub> + z); E = (1 - x, y, <sup>1</sup>/<sub>2</sub> - z). Primed labels refer to secondary orientation.

small cavity. The hexane molecules appear to have a slight preference for the small cavities. A comparison of guests and cavity sizes indicates considerable freedom for motion and dynamic disorder. Symmetrically translated, the orientations found for the guest fill the channel space tightly. This implies a physical mode of sorption as there are only van der Waals interactions with the inner channel surface. We suggest that the two guest orientations described above are the most probable, although it is unlikely that they are the only ones. Neither isopiestic nor X-ray experiments give ideal stoichiometries for the composition, and, therefore, a strict periodicity is not expected.

**Interaction with Alcohols: Inclusion vs Coordination.** In the course of this work we encountered a remarkable phenomenon: the character of the interaction of alcohol with the [CuL<sub>2</sub>] complex switched from chemical coordination to physical sorption inside the channels on going from methanol to higher homologues. This may be rationalized by taking into account that the alcohol molecule has two distinct parts that influence formation of binary compounds with [CuL<sub>2</sub>]. The first, involving the hydroxy group, interacts chemically, and is capable of coordinating to apical sites on the copper atoms of the complex. The other is the hydrophobic portion of the alcohol molecule, conducive to promoting channel formation and filling the same through physical sorption. Whereas the capacity for chemical interaction may be taken as a constant factor, the hydrophobic portion of the molecule increases dramatically on going from methanol to the higher alcohols. The competition between these two factors explains the experimental facts observed very well.

When placing [CuL<sub>2</sub>] under methanol vapor (under conditions of the isopiestic experiment) the blue sample

transforms reversibly to a green powder. The mass increase corresponds to 2 equiv of absorbed methanol, and the X-ray powder pattern test indicates the formation of a new phase, it being neither the  $\alpha$ - nor the  $\beta$ -form. The same product forms by direct crystallization of the complex from a methanol solution. From X-ray structure determination, the product is a bis-methanol complex (Figure 4). Besides square-planar ligation by two bidentate L-units, copper is coordinated apically by two methanol molecules (the whole unit is *trans*-configured). The Cu-O (methanol) distance of 2.47 Å, though longer than the 1.95 Å distance of the main coordination bonds, indicates that methanol undoubtedly is bound chemically so that it can hardly be considered as a guest component. As for the overall structure, the methanol molecule turns out to switch the connecting coordination units into a two-dimensional network that has no space for inclusion. There is hydrogen bonding between the methoxy oxygen and the hydroxy group of neighboring molecules at 2.89 Å (see Table 2 and Figure 4, bottom) resulting in 2-D polymer-like structure.

In an atmosphere of ethanol, blue [CuL<sub>2</sub>] transforms reversibly to an emerald-green powder. The mass increase corresponding to 0.669(5) equiv of ethanol is very near to the <sup>2</sup>/<sub>3</sub> value that would allow one to assume that a  $\beta$ -type inclusion is formed. The X-ray powder pattern test (as well as the color) however indicates that another new, unknown phase is formed. A single-crystal X-ray study of the compound (crystallized from neat ethanol) shows that it is a metal complex without nonbonded (guest) molecules. The structure is complicated, dominated by the packing of weakly coordinating centrosymmetric trimers consisting of three coordination units with the formula {[Cu(EtOH)L<sub>2</sub>]<sub>2</sub> [CuL<sub>2</sub>]}

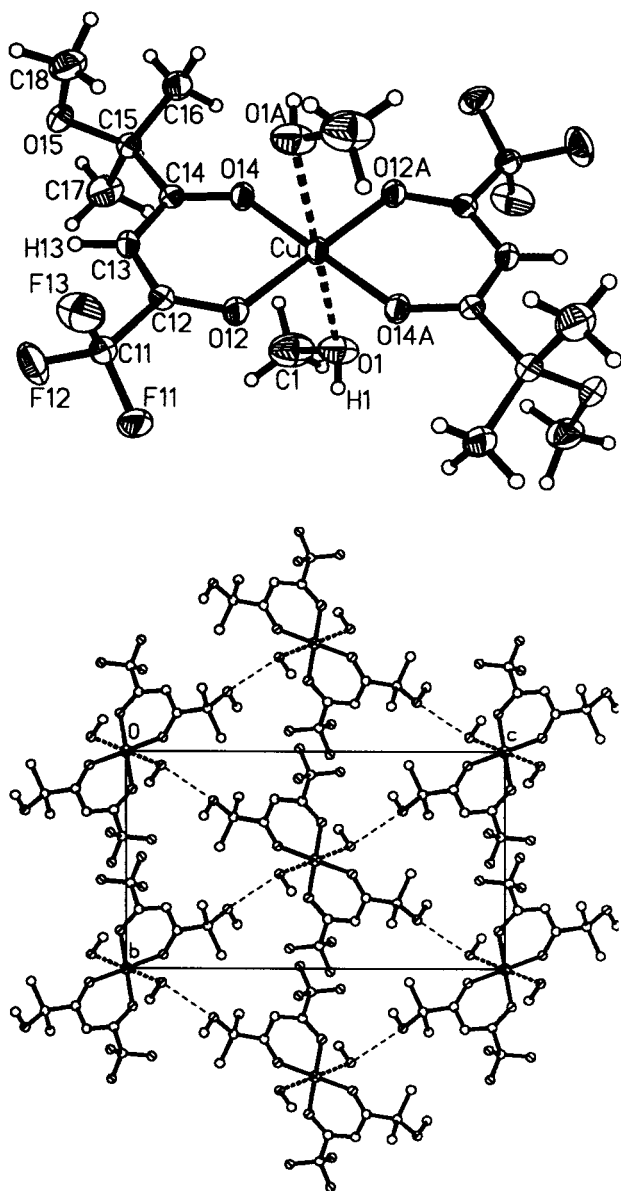


**Figure 4.** Top: Molecule of  $[\text{Cu}(\text{MeOH})_2\text{L}_2]$ . A-labeled atoms are generated by centrosymmetry. Selected bond distances (Å) and angles (deg): Cu–O12, 1.949(1); Cu–O14, 1.951(1); Cu–O1, 2.466(2); O12–Cu–O14, 93.14(5); O14–Cu–O12A, 86.86(5); O12–Cu–O1, 92.04(5); O14–Cu–O1, 96.91(5); Cu–O1–C1, 117.4(2). Bottom: 2-D molecular assembly of the structure. The hydrogen-bonded layer lies perpendicular to the *a*-axis and interacts with the lower and higher layers only by van der Waals interactions. H-atoms are omitted.

(Figure 5). The usual *trans*- $[\text{CuL}_2]$  unit is in the center with typical values for the bond lengths and angles. Two other units coordinate to the central one through methoxy oxygens at 2.56 Å. They are *cis*-configured, and have additional strong coordination of ethanol to copper at distances as short as 2.27 Å. Each trimer connects to two others by additional coordination (see Table 2 and Figure 5, bottom), forming wide bands stretching along the *c*-axis. The whole structure can thus be classified as a 1-D coordination polymer with both *cis* and *trans*  $[\text{CuL}_2]$  bis-chelate units.

In contrast to the lower homologues, the propanols and higher alcohols are included as guests to give  $\beta$ -inclusions with  $[\text{CuL}_2]$  (Scheme 1, eq 2). Thus, this study serves to illustrate the extent to which noncovalent

interactions may govern certain chemical structure-forming processes: enlarging the hydrophobic function of the alcohol molecule in this homologous series leads to a switching from chemical coordination to inclusion through physical sorption. Such a phenomenon merits special attention, as the energies associated with chemical bonding and supramolecular assembly are quite different. Supramolecular chemistry, defined as “chemistry beyond the molecule”, operates with the assumption that during assembly the participating molecules are stable enough to remain intact in all of the processes under consideration. Indeed, individually, noncovalent forces are one to two orders weaker than chemical bonding. However, it is clear that the cumulative effect of many weak interactions may have a significant impact. As illustrated here, this impact can be enough to switch the mode of bond formation, thus re-directing the entire compound formation process. Recently similar observations were reported for some Werner clathrates where van der Waals forces were found to stabilize not only conformations but also molecular isomers and molecules.<sup>12</sup>

The data on compositions and melting parameters for  $\beta$ -inclusions with alcohols are listed in Table 3. These give unequivocal evidence of host matrix specificity with respect to certain alcohols. The structural details of the guests have a significant influence on the composition and/or thermal stability of the resulting inclusions. The most frequently observed guest:host ratio is near to  $2/3$ , the value that corresponds to filling of each wide part of the channel with exactly one guest molecule. In some cases (especially *tert*-butanol and *tert*-amyl alcohol) the quantity of included guest increases dramatically and reaches the ideal stoichiometry. The melting temperatures of the inclusions do not correlate with guest volatility, as probably there also is sensitivity to the quality of guest:host complementarity in the channel cavities. Guest size also turns out to be important for host preferences. The comparison of composition versus size for normal alcohols (Figure 6) makes it necessary to divide the resulting inclusions into two categories: those with stoichiometric filling of cavities (one guest per cavity for propanol, one guest per two cavities for both hexanol and heptanol) and those whose composition does not allow stoichiometric filling. Remarkably, the melting (decomposition) temperature of the stoichiometric inclusions is significantly higher than would be expected from a monotonic increase with hydrocarbon skeletal size. A complementarity of the host matrix as it relates to guest size of certain alcohols is thus observed, and this is rather more pronounced than for

(10) De Gil, E. R.; Kerr, I. S. *J. Appl. Crystallogr.* **1977**, *10*, 315–320.

(11) (a) Manakov, A. Yu.; Lipkowski, J. *J. Inclusion Phenom.* **1997**, *29*, 41–55. (b) Manakov, A. Yu.; Lipkowski, J.; Suwinska, K.; Kitamura, M. *J. Inclusion Phenom.* **1996**, *26*, 1–20. (c) Lavelle, L.; Nassimbeni, L. R. *J. Inclusion Phenom.* **1993**, *16*, 25–54.

(12) (a) Ukraintseva, E. A.; Soldatov, D. V.; Dyadin, Yu. A.; Logvinenko, V. A.; Grachev, E. V. *Mendeleev Commun.* **1999**, 123–125. (b) Ukraintseva, E. A.; Soldatov, D. V.; Logvinenko, V. A.; Dyadin, Yu. A. *Mendeleev Commun.* **1997**, 102–104. (c) Soldatov, D. V.; Dyadin, Yu. A.; Ukraintseva, E. A.; Kolesov, B. A.; Logvinenko, V. A. *J. Inclusion Phenom.* **1996**, *26*, 269–280. (d) Dyadin, Yu. A.; Soldatov, D. V.; Logvinenko, V. A.; Lipkowski, J. *J. Coord. Chem.* **1996**, *37*, 63–75. (e) Lipkowski, J.; Soldatov, D. V.; Kislykh, N. V.; Pervukhina, N. V.; Dyadin, Yu. A. *J. Inclusion Phenom.* **1994**, *17*, 305–316. (f) Dyadin, Yu. A.; Kislykh, N. V. *Mendeleev Commun.* **1991**, 134–136.

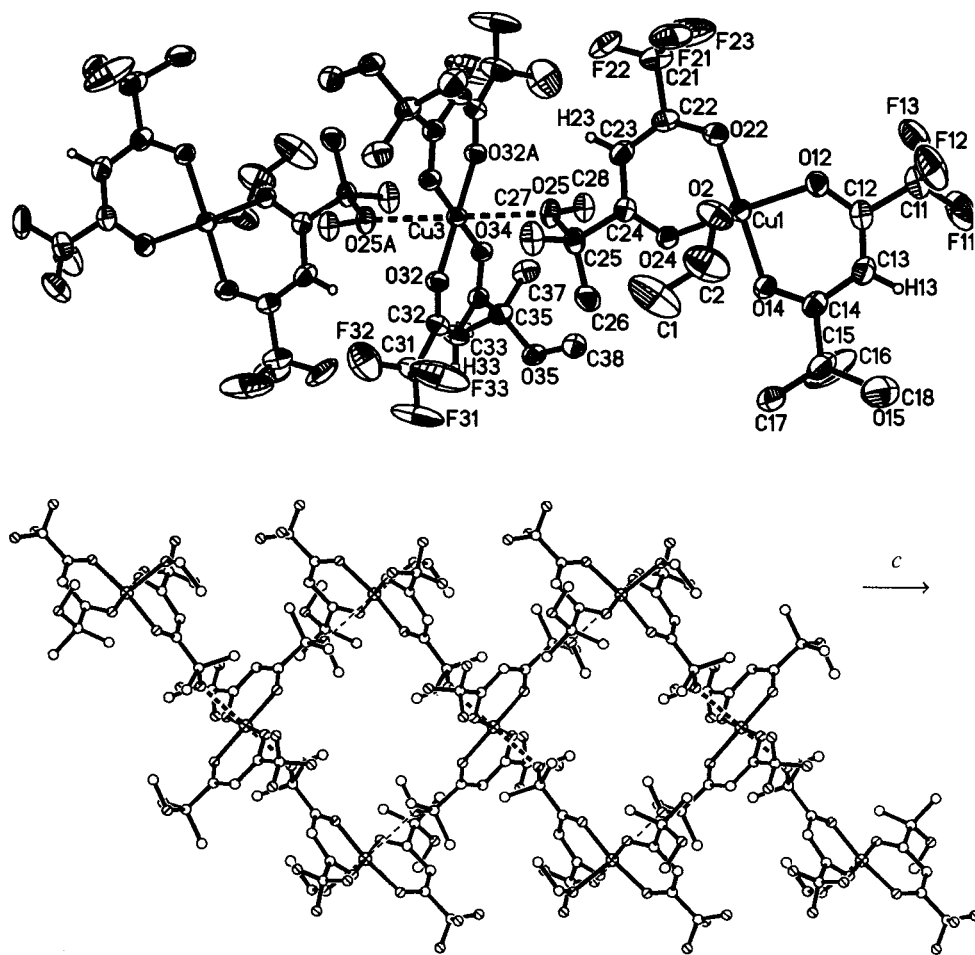


**Figure 5.** Top: Molecular associate  $\{[\text{Cu}(\text{EtOH})\text{L}_2]_2 [\text{CuL}_2]\}$ . A-labeled atoms are generated by centrosymmetry. Methyl, methylene, and hydroxy H-atoms are omitted for clarity. Selected bond distances (Å) and angles (deg): Cu1–O12, 1.938(1); Cu1–O14, 1.940(1); Cu1–O2, 2.265(2); O12–Cu1–O14, 92.54(5); O12–Cu1–O22, 88.28(5); O14–Cu1–O24, 85.90(5); O22–Cu1–O24, 92.39(5); O12–Cu1–O2, 96.05(6); O14–Cu1–O2, 94.14(6); O22–Cu1–O2, 91.80(6); O24–Cu1–O2, 92.37(6); Cu–O2–C2, 130.6(2); Cu3–O32, 1.929(1); Cu3–O34, 1.933(1); Cu3–O25, 2.556(1); O32–Cu3–O34, 92.40(5); O34–Cu3–O32A, 87.60(5); O32–Cu3–O25, 96.07(5); O34–Cu3–O25, 89.81(4). Bottom: 1-D molecular assembly of the structure. Shown is the fragment of the polymer band that lies along the  $c$ -axis and interacts with neighboring bands only by van der Waals interactions. H–Atoms are omitted.

**Table 3. Compositions and Thermal Stability for Addition Products of Alcohols to  $[\text{CuL}_2]$**

alcohol	quantity of sorbed alcohol			method <sup>a</sup>	melting parameters <sup>b</sup>	
	mass %	mol ( $x$ )	exp $t$ , °C		$t$ , °C	type
Coordination Compounds						
methanol	13.5(1)	2.04(2)	20	C	67	incongruent
ethanol	6.34(5)	0.669(5)	20	C	70	incongruent
$\beta$ -Inclusions						
<i>n</i> -propanol	8.10(5)	0.655(4)	20	C	114	incongruent
isopropanol	8.17(3)	0.660(3)	20	C	124.5	incongruent
<i>n</i> -butanol	7.46(4)	0.489(3)	20	C	117	incongruent
2-butanol, racemic	9.82(4)	0.644(3)	20	C	118	incongruent
2-butanol, <i>d</i> -isomer	9.72(5)	0.637(3)	20	C	118	incongruent
2-butanol, <i>l</i> -isomer	9.82(3)	0.644(2)	20	C	118	incongruent
<i>tert</i> -butanol	10.31(8)	0.676(5)	~25	C	135.5	incongruent
<i>n</i> -pentanol	7.67(3)	0.423(2)	20	C	126	incongruent
2-pentanol	7.49(3)	0.413(2)	20	C	121	incongruent
<i>tert</i> -amyl alcohol	12.07(3)	0.665(2)	20	C	116.5	incongruent
neopentyl alcohol	9.45(3)	0.521(2)	20	C	133.5	incongruent
<i>n</i> -hexanol	7.17(3)	0.341(2)	50	C	138.5	incongruent
<i>n</i> -heptanol	8.07(3)	0.337(2)	50	C	143	incongruent
<i>n</i> -octanol	8.07(3)	0.301(2)	50	C	142	incongruent

<sup>a</sup> See Experimental Part for description. <sup>b</sup> Pure  $[\text{CuL}_2]$  host in its  $\alpha$ -form melts congruently at 157 °C.

the hydrocarbons (cf. Figure 1). Thus, the host matrix is able to recognize definite species among homologues, especially if they are polar.

The structure of nonstoichiometric inclusions is likely to be similar to the structure described above for the hexane inclusion. As a main difference, we would



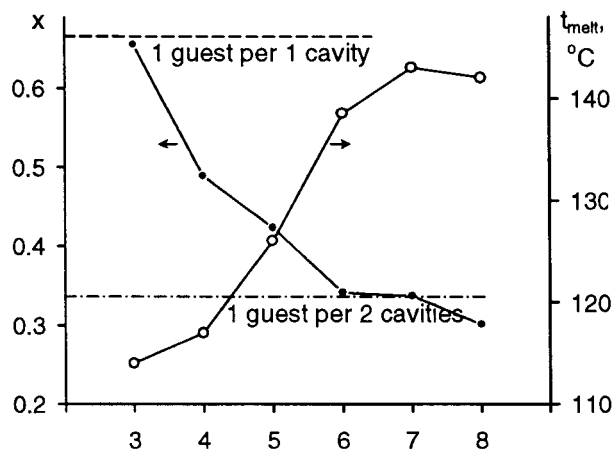


**Figure 6.** Guest–host mole ratios  $x$  (solid circles, left axis) and melting temperatures (open circles, right axis) versus number of guest carbons  $y$  for the  $\beta$ -[CuL<sub>2</sub>] $\cdot$  $x$ ( $n$ -C <sub>$y$</sub> H <sub>$2y+1$</sub> OH) inclusions.

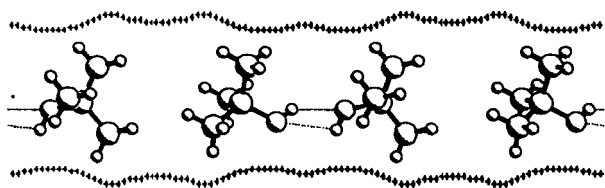


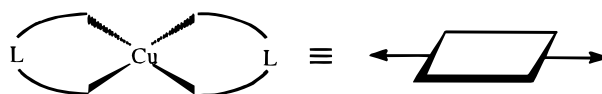
**Figure 7.** Location of guest dimers in  $\beta$ -[CuL<sub>2</sub>] $\cdot$  $2/3$ (*tert*-butanol) (see notations to Figure 3). Two symmetry-related guest molecules are connected through hydrogen bonding at an O–O distance of 2.58(2) Å.

suggest the formation of hydrogen-bonded pairs of guest species and a greater orientation of guests inside channels.

An example of a stoichiometric structure is given by the X-ray study of the inclusion with *tert*-butanol. As to the host structure, it is very similar to the hexane inclusion mentioned above. The main structural parameters for the [CuL<sub>2</sub>] unit in each structure coincide within experimental error. The basic building unit thus remains more or less unchanged. At the same time, there are slight differences in the intermolecular assembly. As one can see from Table 2, this is indicated by changes in the additional coordination bond lengths. Also, in the *tert*-butanol inclusion, disorder over two orientations is observed in the –C(OCH<sub>3</sub>)(CH<sub>3</sub>)<sub>2</sub> fragment. The methoxy oxygen associated with a secondary orientation (the occupancy is 10%, the atoms are labeled with a prime in Table 2) does not ligate well to the copper of a neighboring unit, but it does form a shorter intramolecular hydrogen bond to the >C–H group of the chelate ring. Analogous disorder was observed previously for the benzene inclusion, as well as for the guest-free  $\alpha$ -form of the title complex.<sup>6</sup> This kind of disorder is important and likely to be responsible for some flexibility of the  $\beta$ -matrix, allowing its expansion, if necessary. The most pronounced difference with the hexane inclusion is, however, in the arrangement of the guest species in the channel space. The guest-to-host ratio of exactly  $2/3$  follows from the stoichiometric filling of available cavities (Figure 7). Guest molecules reside on both sides of the large cavity, extending their hydroxy groups into the small cavity to form hydrogen bonds to a molecule located in the adjacent large cavity. So, guest species are associated in pairs. This model may be

applied as well to other stoichiometric inclusions listed in Table 3. The specific orientation of guest molecules, including their particular conformation and arrangement relative to the host matrix and neighboring guests, provide the basis for spectroscopic research into templates<sup>13</sup> and templated polymerization.<sup>14</sup>

**On Design of 3-D Microporous Sponges Using Bis-chelate Blocks.** The above structural data for binary compounds between [CuL<sub>2</sub>] and alcohols illustrate how varying the size of the hydrophobic part of the guest induces the formation of either 1-D, or 2-D, or 3-D polymers. Generally speaking, the [CuL<sub>2</sub>] molecule represents a coordinatively unsaturated bidentate building block, or supramolecular synthon, with two pairs of acceptor and donor sites oppositely directed within each pair:



Note that the coordinating alcohol molecule does not change this situation, as the hydroxy group is able to link to methoxy oxygen using hydrogen bonding. Theoretically, the self-assembly of such units may well lead to 1-D, 2-D, and 3-D structures, but in reality the 3-D type is rarely encountered. The closest analogues of the title complex, [CuL<sup>1</sup>],<sup>15</sup> [CuL<sup>2</sup>],<sup>15</sup> and [CuL<sup>3</sup>],<sup>16</sup> form pure molecular structures without external bonding (see Scheme 2).<sup>17</sup> In all three structures, alkoxy oxygen forms an intramolecular hydrogen bond to a >C–H group, as for the compounds studied in this work (Table 2), but they do not coordinate to Cu(II), leaving it in a square environment. With the analogous enamine ligand, the 1-D coordination polymer [CuL<sup>4</sup>]<sub>2</sub> was obtained.<sup>18</sup>

A number of coordination and hydrogen-bonded architectures was designed using metal bis-chelates with deprotonated nitroxide radical derivatives L<sup>5</sup>–L<sup>10</sup>. These include  $\alpha$ - and  $\beta$ -[NiL<sup>5</sup>],<sup>19</sup>  $\beta$ -[CoL<sup>5</sup>],<sup>20</sup> [Ni(H<sub>2</sub>O)<sub>2</sub>L<sup>5</sup>],<sup>21</sup> [Ni(*n*-BuOH)<sub>2</sub>L<sup>5</sup>],<sup>22,23</sup> [Ni(*i*-BuOH)<sub>2</sub>L<sup>5</sup>],<sup>23</sup> [Co(MeOH)<sub>2</sub>-

(13) For a general review of this technique see Davies, J. E. D. In *Inclusion Compounds*; Atwood, J. L., Davies, J. E. D., MacNicol, D. D., Eds.; Academic Press: London, 1984; Vol. 3, pp 37–68.

(14) Hollingsworth, M. D.; Harris, K. D. M. In *Comprehensive Supramolecular Chemistry*; MacNicol, D. D., Toda, F., Bishop, R., Eds.; Pergamon: Oxford, 1996; Vol. 6, pp 177–237, and references from 167 to 210 therein.

(15) Baydina, I. A.; Gromilov, S. A.; Stabnikov, P. A.; Vasil'ev, A. D. *Zh. Strukt. Khim.* **1997**, *38*, 954–959 (in Russian).

(16) Baydina, I. A.; Gromilov, S. A.; Stabnikov, P. A.; Prokhorova, S. A. *Zh. Strukt. Khim.* **1994**, *35* (No. 6), 169–175 (in Russian).

(17) These  $\beta$ -diketonates were studied extensively as precursors for CVD (chemical vapor deposition) processes. For this purpose it was necessary to produce highly volatile mononuclear complexes, but special attempts to obtain multidimensional structures were not made until now. For the relevant literature see: (a) Krisyuk, V. V.; Sysyov, S. V.; Fedotova, N. E.; Igumenov, I. K.; Grigorieva, N. V. *Thermochimica Acta* **1997**, *307*, 107–115. (b) Turgambaeva, A. E.; Bykov, A. F.; Igumenov, I. K. *J. Phys. IV, Coll. C5, supplement au J. Phys. II* **1995**, *5*, 221–228. (c) Gerasimov, P. A.; Gerasimova, A. I.; Arkhipov, I. K.; Igumenov, I. K. *Russ. J. Appl. Chem.* **1993**, *66* (No. 8; Part 2), 1410–1412; in Russian version 1807–1810.

(18) Baydina, I. A.; Gromilov, S. A.; Stabnikov, P. A.; Vasil'ev, A. D. *Zh. Strukt. Khim.* **1997**, *38*, 136–141 (in Russian).

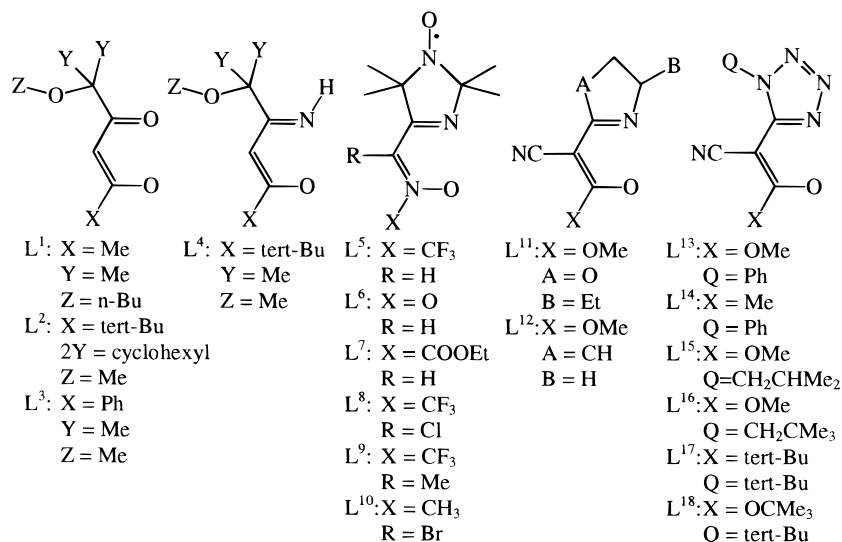
(19) Ovcharenko, V. I.; Romanenko, G. V.; Ikorskii, V. N.; Musin, R. N.; Sagdeev, R. Z. *Inorg. Chem.* **1994**, *33*, 3370–3381.

(20) Romanenko, G. V.; Podbereskaya, N. V.; Ovcharenko, V. I. *Zh. Neorg. Khim.* **1992**, *37*, 1525–1530 (in Russian).

(21) Ovcharenko, V. I.; Vostrikova, K. E.; Podoplelov, A. V.; Sagdeev, R. Z.; Romanenko, G. V.; Ikorskii, V. N. *Polyhedron* **1994**, *13*, 2781–2792.



Scheme 2



$L^6$ ],<sup>24</sup>  $[\text{CoL}^7_2]$  and  $[\text{CuL}^7_2]$ ,<sup>25</sup>  $[\text{Ni}(\text{MeOH})_2\text{L}^5_2]$  and its Co counterpart,<sup>26</sup>  $[\text{Ni}(\text{MeOH})_2\text{L}^8_2]$  and its Co counterpart,<sup>26</sup>  $[\text{Ni}(\text{MeOH})_2\text{L}^9_2]$ ,<sup>26</sup> and  $[\text{Ni}(\text{MeOH})_2\text{L}^{10}_2]$ .<sup>27</sup> The general feature in the series is that nitroxide oxygens connect to neighboring units through either coordination to the metal center or hydrogen bonding to the alcohol hydroxy group. Although most efforts were directed at creation of 3-D polymers in order to obtain special magnetic properties, all complexes listed are 2-D polymers.

Saalf Frank et al. reported a series of bis-chelates with tridentate ligands  $L^{11}$ – $L^{18}$ . For these, the nitrogen of the nitrile group plays the role of the bridging connector to neighboring building blocks. Whereas  $[\text{Cu}(\text{MeOH})\text{L}^{11}_2]$  is mononuclear, removing methanol in a chloroform medium gave the solvate  $[\text{CuL}^{11}_2] \cdot 2(\text{CHCl}_3)$  with a chiral 1-D coordination polymer.<sup>28</sup>  $[\text{CuL}^{13}_2]$ ,<sup>29,30</sup> and  $[\text{Zn}(\text{MeOH})_2\text{L}^{14}_2]$ <sup>29</sup> are mononuclear,  $[\text{CuL}^{15}_2]$  and  $[\text{CuL}^{16}_2]$  are 1-D,<sup>31</sup>  $[\text{CuL}^{12}_2]$ ,<sup>32</sup>  $[\text{CuL}^{14}_2]$  and  $[\text{CuL}^{17}_2]$ <sup>29</sup> are 2-D, and  $[\text{CuL}^{18}_2] \cdot (\text{CH}_2\text{Cl}_2)$ <sup>33</sup> is a 3-D coordination polymer accommodating guest methylene chloride. The latter

resembles the title  $\beta$ -matrix in terms of structural parameters but it is the only 3-D structure from the literature cited here. This analysis of reported architectures illustrates that the problem of using metal bis-chelates to create 3-D supramolecular assemblies with pore space is neither easy nor obvious, and a thorough analysis of all available factors is necessary.

**Range of Components for Inclusion.** To investigate the propensity of the title complex for including different classes of organic compounds the so-called wetting probe was used (Scheme 1, reactions 1 or 6). Pure  $\alpha$ -phase of the  $[\text{CuL}_2]$  was wetted with the corresponding liquid compound, and a powder diffraction experiment was performed on this wetted sample. The results obtained are listed in Table 4. For the overwhelming majority of candidates used, full transformation to the  $\beta$ -form was observed characteristic of the inclusion reaction 1, Scheme 1.

Typically, the transformation was complete by the time (as short as 1 min) analysis started.

However, in a number of cases, the inclusion process was delayed significantly, and for some it did not occur at all unless special procedures were used. This situation arose because of a kinetic barrier between the dense and open polymorphs of the host complex. From our previous study,<sup>6</sup> the dense  $\alpha$ -form has half of the copper bis-chelates present as the *cis* isomer, whereas in the  $\beta$  form they are all *trans* isomers. The phase change therefore depends on the isomerization of half of the chelate building blocks, requiring the breaking of coordination bonds around the metal center. This process is clearly affected by the presence of a sorbent acting as a catalyst. It is likely that many sorbents play a double role in the clathrate formation process, that of stabilizing the empty  $\beta$ -form (thermodynamic action) and catalyzing the *cis*–*trans* isomerization necessary for phase interconversion (kinetic aspect). However, there are sorbents capable of being included, but without the ability to induce  $\alpha$ -to- $\beta$  interconversion. One example is that of paraffin oil, which does not react with  $\alpha$ - $[\text{CuL}_2]$  at all on contact, and only small quantities of the  $\beta$ -phase form in the course of prolonged grinding of the mixture. On the other hand there are also sorbents that are not capable of inclusion because of their large

(22) Romanenko, G. V.; Podberezskaya, N. V. *Zh. Strukt. Khim.* **1993**, *34* (No. 2), 119–125 (in Russian).

(23) Romanenko, G. V.; Ikorskii, V. N.; Fokin, S. V.; Ovcharenko, V. I. *Zh. Strukt. Khim.* **1997**, *38*, 930–945 (in Russian).

(24) Ovcharenko, V. I.; Ikorskii, V. N.; Romanenko, G. V.; Reznikov, V. A.; Volodarskii, L. B. *Inorg. Chim. Acta* **1991**, *187*, 67–72.

(25) Romanenko, G. V.; Podberezskaya, N. V. *Zh. Strukt. Khim.* **1992**, *33* (No. 1), 93–99 (in Russian).

(26) (a) Ikorskii, V. N.; Romanenko, G. V.; Sygurova, M. K.; Ovcharenko, V. I.; Lanfranc de Paunthou, F.; Rey, P.; Reznikov, V. A.; Podoplelov, A. V.; Sagdeev, R. Z. *Zh. Strukt. Khim.* **1994**, *35* (No. 4), 76–90 (in Russian). (b) Ovcharenko, V. I.; Ikorskii, V. N.; Romanenko, G. V.; Sagdeev, R. Z.; Lanfranc de Paunthou, F.; Rey, P. *Synth. Met.* **1997**, *85*, 1639–1642.

(27) Sygurova, M. K.; Romanenko, G. V.; Vostrikova, K. E.; Vishnevetskaya, L. A.; Podberezskaya, N. V. *Zh. Strukt. Khim.* **1995**, *36*, 941–947 (in Russian).

(28) Saalf Frank, R. W.; Decker, M.; Hampel, F.; Peters, K.; Schnering, H. G. *Chem. Ber./Recueil* **1997**, *130*, 1309–1313.

(29) Saalf Frank, R. W.; Harbig, R.; Struck, O.; Peters, E. M.; Peters, K.; Schnering, H. G. *Z. Naturforsch. B* **1996**, *51*, 399–408 (in German).

(30) Peters, K.; Peters, E. M.; Schnering, H. G.; Saalf Frank, R. W.; Struck, O. *Z. Kristallogr.* **1995**, *210*, 547.

(31) Saalf Frank, R. W.; Harbig, R.; Struck, O.; Hampel, F.; Peters, E. M.; Peters, K.; Schnering, H. G. *Z. Naturforsch. B* **1997**, *52*, 125–134 (in German).

(32) Saalf Frank, R. W.; Struck, O.; Peters, K.; Schnering, H. G. *Chem. Ber.* **1993**, *126*, 837–840 (in German).

(33) Saalf Frank, R. W.; Struck, O.; Nunn, K.; Lurz, C. J.; Harbig, R.; Peters, K.; Schnering, H. G.; Bill, E.; Trautwein, A. X. *Chem. Ber.* **1992**, *125*, 2331–2335 (in German).

**Table 4.  $\alpha$ -[CuL<sub>2</sub>] Complex Behavior on Wetting with Organic Substances (Wetting Probe)<sup>a</sup>**

formation of $\beta$ -[CuL <sub>2</sub> ] $\cdot$ $\alpha$ G inclusion compound: Scheme 1, reaction 1 (no change in color; powder X-ray test indicates $\alpha$ -to- $\beta$ conversion)	formation of [CuG <sub>x</sub> L <sub>2</sub> ] coordination compound: Scheme 1, reaction 6a (blue-to-green change in color; powder X-ray test indicates forming new phase, neither $\alpha$ nor $\beta$ )	no interaction (no changes, neither in color nor of powder X-ray pattern)
<b>Hydrocarbons and Their Halo-Derivatives</b>		
normal paraffins from C5 to C16*; those with methyl-, ethyl-, and halo- substituents; paraffin oil,* (white, code 2044); <sup>b</sup> methylene chloride, CH <sub>2</sub> Cl <sub>2</sub> ; chloroform, CHCl <sub>3</sub> ; carbon tetrachloride, CCl <sub>4</sub> ; bromoform, CHBr <sub>3</sub> ; cyclopentane,* cyclo-C <sub>5</sub> H <sub>10</sub> ; cyclohexane,* cyclo-C <sub>6</sub> H <sub>12</sub> ; cycloheptane,* cyclo-C <sub>7</sub> H <sub>14</sub> ; cyclooctane,* cyclo-C <sub>8</sub> H <sub>16</sub> ; isoprene, CH <sub>2</sub> =CHC(CH <sub>3</sub> )=CH <sub>2</sub>		
<b>Alcohols</b>		
1-propanol, C <sub>3</sub> H <sub>7</sub> OH; 2-propanol, CH <sub>3</sub> CH(OH)CH <sub>3</sub> ; 1-butanol, C <sub>4</sub> H <sub>9</sub> OH; 2-butanol, C <sub>2</sub> H <sub>5</sub> CH(OH)CH <sub>3</sub> (including both optical isomers and racemate); <i>tert</i> -butanol, (CH <sub>3</sub> ) <sub>3</sub> COH; 1-pentanol, C <sub>5</sub> H <sub>11</sub> OH; 2-pentanol, C <sub>3</sub> H <sub>7</sub> C(OH)CH <sub>3</sub> ; <i>tert</i> -amyl alcohol, C <sub>2</sub> H <sub>5</sub> C(OH)(CH <sub>3</sub> ) <sub>2</sub> ; neopentyl alcohol, (CH <sub>3</sub> ) <sub>3</sub> CCH <sub>2</sub> OH; 1-hexanol, C <sub>6</sub> H <sub>13</sub> OH; 1-heptanol, C <sub>7</sub> H <sub>15</sub> OH; 1-octanol, C <sub>8</sub> H <sub>17</sub> OH	methanol,* CH <sub>3</sub> OH; ethanol, C <sub>2</sub> H <sub>5</sub> OH	
<b>Diols</b>		
1,7-heptanediol,* HOC <sub>7</sub> H <sub>14</sub> OH	ethylene glycol,* HOCH <sub>2</sub> CH <sub>2</sub> OH; 1,3-propanediol,* HO-(CH <sub>2</sub> ) <sub>3</sub> -OH	2,4-pentanediol (mix. isomers), CH <sub>3</sub> C(OH)CH <sub>2</sub> C(OH)CH <sub>3</sub>
<b>Aldehydes, Ketones, and Diketones</b>		
propionaldehyde, CH <sub>3</sub> CH <sub>2</sub> CHO; acetone, CH <sub>3</sub> COCH <sub>3</sub> ; diisopropyl ketone, (CH <sub>3</sub> ) <sub>2</sub> CHCOCH(CH <sub>3</sub> ) <sub>2</sub> ; cyclopropylmethyl ketone, cyclo-C <sub>3</sub> H <sub>5</sub> COCH <sub>3</sub> ; acetylacetone, CH <sub>3</sub> COCH <sub>2</sub> COCH <sub>3</sub> ; acetonylacetone,* CH <sub>3</sub> COC <sub>2</sub> H <sub>4</sub> COCH <sub>3</sub>		
<b>Ethers</b>		
diethyl ether, C <sub>2</sub> H <sub>5</sub> OC <sub>2</sub> H <sub>5</sub> ; isopropyl ether, (CH <sub>3</sub> ) <sub>2</sub> CHOCH(CH <sub>3</sub> ) <sub>2</sub> ; <i>tert</i> -butyl methyl ether, (CH <sub>3</sub> ) <sub>3</sub> COCH <sub>3</sub> ; diphenyl ether, C <sub>6</sub> H <sub>5</sub> OC <sub>6</sub> H <sub>5</sub> ; 2,2'-dimethoxypropane, (CH <sub>3</sub> ) <sub>2</sub> C(OCH <sub>3</sub> ) <sub>2</sub> ; oxetane, cyclo-C <sub>3</sub> H <sub>6</sub> O; $\beta$ -butirolactone (racemic), CH <sub>3</sub> -cyclo-C <sub>3</sub> H <sub>5</sub> O; tetrahydrofuran, cyclo-C <sub>4</sub> H <sub>8</sub> O; 1,3-dioxolane, cyclo-C <sub>2</sub> H <sub>4</sub> OCH <sub>2</sub> O; 1,3-dioxane, cyclo-C <sub>3</sub> H <sub>6</sub> OCH <sub>2</sub> O; 3,4-dihydro-2 <i>H</i> -pyran, cyclo-C <sub>3</sub> H <sub>6</sub> C <sub>2</sub> H <sub>2</sub> O	1,4-dioxane, cyclo-C <sub>2</sub> H <sub>4</sub> OC <sub>2</sub> H <sub>4</sub> O	
<b>Esters and Ethers of Mineral Acids</b>		
methylformate, HCOOCH <sub>3</sub> ; methyl acetate, CH <sub>3</sub> COOCH <sub>3</sub> ; amyl acetate, CH <sub>3</sub> COOC <sub>4</sub> H <sub>9</sub> CH <sub>3</sub> ; diethyl carbonate, (C <sub>2</sub> H <sub>5</sub> O) <sub>2</sub> CO; dimethyl sulfate, (CH <sub>3</sub> O) <sub>2</sub> SO <sub>2</sub>	trimethyl phosphate, (CH <sub>3</sub> O) <sub>3</sub> PO	
<b>Anhydrides, Acids, and Amides</b>		
acetic anhydride,* (CH <sub>3</sub> CO) <sub>2</sub> O; acetic acid, CH <sub>3</sub> COOH; 2-ethylhexanoic acid,* CH <sub>3</sub> (CH <sub>2</sub> ) <sub>3</sub> CH(C <sub>2</sub> H <sub>5</sub> )COOH;	dimethylformamide, HCON(CH <sub>3</sub> ) <sub>2</sub>	
<b>Nitriles and Dinitriles</b>		
acetonitrile,* CH <sub>3</sub> CN; acrylonitrile, H <sub>2</sub> C=CHCN; 1,4-dicyanobutane,* NC-C <sub>2</sub> H <sub>4</sub> -CN		
<b>Amines and Heterocyclic Amines</b>		
	diethylamine, (C <sub>2</sub> H <sub>5</sub> ) <sub>2</sub> NH; triethylamine, (C <sub>2</sub> H <sub>5</sub> ) <sub>3</sub> N; triethanolamine, (HOCH <sub>2</sub> CH <sub>2</sub> ) <sub>3</sub> N; pyridine, C <sub>5</sub> H <sub>5</sub> N and its derivatives; quinoline, C <sub>9</sub> H <sub>7</sub> N	

**Table 4.  $\alpha$ -[CuL<sub>2</sub>] Complex Behavior on Wetting with Organic Substances (Wetting Probe)<sup>a</sup>**

formation of $\beta$ -[CuL <sub>2</sub> ] $\cdot$ xG inclusion compound: Scheme 1, reaction 1 (no change in color; powder X-ray test indicates $\alpha$ -to- $\beta$ conversion)	formation of [CuG <sub>x</sub> L <sub>2</sub> ] coordination compound: Scheme 1, reaction 6a (blue-to-green change in color; powder X-ray test indicates forming new phase, neither $\alpha$ nor $\beta$ )	no interaction (no changes, neither in color nor of powder X-ray pattern)
	Aromatics	
benzene, C <sub>6</sub> H <sub>6</sub> and its 20 derivatives listed in ref 6 (bearing F-, Cl-, Br-, I-, -CH <sub>3</sub> , -CF <sub>3</sub> , -CCl <sub>3</sub> , -NO <sub>2</sub> , -CHO, -C <sub>2</sub> H <sub>5</sub> , -cyclo-CH(CH <sub>2</sub> ) <sub>2</sub> , -C <sub>3</sub> H <sub>7</sub> , -C(CH <sub>3</sub> ) <sub>3</sub> , -F and -CH <sub>3</sub> (para), -F and -OCH <sub>3</sub> (para), di-(CH <sub>3</sub> ) (ortho, meta and para), di-Cl (para) and hexa-F functions)		mesitylene, 1,3,5-(CH <sub>3</sub> ) <sub>3</sub> -C <sub>6</sub> H <sub>3</sub>
	Others	
nitromethane,* CH <sub>3</sub> NO <sub>2</sub> ; carbon disulfide, CS <sub>2</sub> ; tetramethyl orthosilicate, (CH <sub>3</sub> O) <sub>4</sub> Si; triethylsilane,* (C <sub>2</sub> H <sub>5</sub> ) <sub>3</sub> SiH	dimethyl sulfoxide, (CH <sub>3</sub> ) <sub>2</sub> SO	water, H <sub>2</sub> O; triisopropylsilane, {(CH <sub>3</sub> ) <sub>2</sub> CH} <sub>3</sub> SiH; 2-acetylthiophene, cyclo-SC <sub>4</sub> H <sub>3</sub> -COCH <sub>3</sub>

<sup>a</sup> Comments: The asterisks (\*) indicates that the conversion is kinetically delayed and requires mesitylene catalysis and/or prolonged grinding. One more (fourth) possibility was the irreversible destruction of the [CuL<sub>2</sub>] material (irreversible changes in color; powder X-ray test indicates loss of crystallinity); the mode was observed, e.g., for ethanethiol, C<sub>2</sub>H<sub>5</sub>SH. <sup>b</sup> From Baker & Adamson, General Chemical Division, Morristown, NJ.

size but that are able to induce the  $\alpha$ -to- $\beta$  interconversion successfully, thus acting as catalysts. Mesitylene is a very convenient choice for that. So, addition of a little mesitylene to a mixture of  $\alpha$ -[CuL<sub>2</sub>] and paraffin oil completes the reaction within minutes, suggesting a general approach to process control.

As evident from Table 4, the variety of guests that can be included is extremely wide. Among the more than 100 guests there are normal, branched, and cyclic hydrocarbons, their F, Cl, Br, I, and S derivatives, alcohols, ethers, esters, ethers of mineral acids, acid anhydrides and acids, aldehydes, ketones, compounds with nitro, amide, and cyano functions. The largest molecules capable of inclusion are some components of paraffin oil, cyclooctane, diphenyl ether, and tetramethyl orthosilicate, and these are likely to define the upper limits for guest dimensions. Mesitylene and triisopropylsilane exceed this limit and thus are not included.

Clearly, the host material is a versatile sorbent for many classes of organic compounds to which it behaves in a stable manner. Inclusion of reactive species such as the unsaturated organics, acetic anhydride and compounds with aldehyde and nitrile functions suggest the possibility of using the matrix channels for directed synthesis. For instance, inclusion of monomers such as isoprene and lactones would allow templated isomerization inside the matrix. Inclusion of components such as carbonic acids, capable of dissociation, might allow processes involving ion exchange and the creation of useful new materials.

Compounds with strong donor groups such as amines, or compounds with oxygen-containing functions, also are capable of coordinating to the copper center resulting in the loss of the inclusion function of the host material. In many cases this is easily reversed and may also be used for process control by temporarily "switching off" guest adsorption (Scheme 1, reaction 6b). Table 4 shows that there is always competition between the tendency of a potential donor to ligate to a copper center and the tendency of the hydrocarbon part to be sorbed into the hydrophobic channel. Water gives yet a third possibility, as it does not react with the complex either as ligand or as guest. This shows that the energetically favorable hydrogen bonds present in neat water are not broken.<sup>34</sup>

At the same time, the preservation of hydrogen bonded dimers is likely to be responsible for inclusion of acetic acid, whereas ligation to copper would require their breaking. Among these three tendencies, a delicate balance is demonstrated by the diols. The simplest, ethylene glycol, and propanediol do coordinate to copper, pentanediols do not react at all, while heptanediol reacts, but as a guest promoting formation of the open  $\beta$ -form. In generalizing these tendencies, the dioxanes exemplify a case where isomerism is seen to be important, as 1,3-dioxane causes  $\beta$ -clathrate formation, whereas 1,4-dioxane gives a coordination compound.

## Conclusion

The construction of microporous frameworks from organically based building units is one of the significant achievements of supramolecular chemistry and an attractive prospect for the future. Mimicking some of the basic properties of inorganic materials such as the zeolites, they present many new possibilities and even greater variability. The processes involved in their formation may be controlled quite effectively because of the simplicity of initiating self-assembly, and the reverse process can be achieved merely by adding appropriate solvents or changing pH. Although most of these materials have been discovered by chance, there is every reason to believe that the scope for such systems will be vast, and that the rational design and synthesis of new systems is just a matter of time. The material studied here reveals both an extremely high versatility with respect to the range of included species and a remarkable robustness of the host matrix, thus allowing a near-endless variation of guest type. At the same time, the present study elucidates the sensitive balance of factors leading to this supramolecular construction. A salient example is given by the chemical homologues methanol, ethanol, and propanol that are able to direct self-assembly to the formation of 1-D, 2-D, or 3-D coordination polymers just because of an increment in

(34) Exposure of the outgassed  $\beta$ -[CuL<sub>2</sub>] to water vapor resulted in little weight change, suggesting sorption was negligible. Allison and Barrer<sup>5k</sup> reported analogous observations for the first organic zeolite analogues which differ from the usual zeolites by their propensity to take in sorbents of a hydrophobic nature.



the number of methylene groups. Even within the same 3-D matrix pore, spatial restrictions reveal crucial differences in the nature of the inclusions within these homologous series. The title material merits special attention because it presents a number of properties rarely or never observed before for systems of this nature: as a 3-D polymer constructed of a (2 + 2) supramolecular synthon it preserves its pore space robustly; as a new channeled matrix it displays unique spatial properties; it shows catalytic switching between dense and open forms; it displays solid-phase interconversions in an atmosphere of aliphatic hydrocarbon gases. In this way, new ideas and design concepts for 21st century materials become apparent.

### Experimental Section

**Starting Compounds.** 1,1,1-Trifluoro-5,5-dimethyl-5-methoxyacetone (HL) and the [CuL<sub>2</sub>] complex were prepared as described before.<sup>6,35</sup> Crystalline adducts were prepared from solutions of  $\alpha$ -[CuL<sub>2</sub>] in the respective solvents, by cooling (*n*-hexane, *tert*-butanol), or by slow evaporation (methanol, ethanol). Gases used (methane, ethane, propane, *n*-butane, neopentane, and methyl bromide) were of 99.5% purity or better (Matheson Gas Products, Canada); liquid reagents were of reagent grade quality or better.

**Synthesis and Analysis of Clathrates by the Isopiestic Method.** In this method<sup>36</sup> the reaction of solid host with guest vapors occurs at constant temperature and constant guest vapor pressure until constant mass is obtained. For these experiments  $\alpha$ -[CuL<sub>2</sub>] of high chemical and phase purity was prepared.<sup>6</sup> To prepare the empty  $\beta$ -form of the complex, the  $\alpha$ -form was treated with methyl bromide, followed by complete evacuation (Scheme 1, reactions 2 and 3).<sup>6</sup> The  $\beta$ -form was prepared not more than 24 h before the experiments, and it was checked for phase purity before each experiment. The experiments were conducted in three different variations.

In *Method A* (Scheme 1, reaction 4) the TGA 2050 thermogravimetric analyzer (TA Instruments, RMX-Based Operating System) was adapted. Before each measurement, the purge gas system was thoroughly cleaned of volatile impurities with a nitrogen stream. Experiments were performed in the isothermal (20 °C) regime. A sample of ~20 mg of empty  $\beta$ -[CuL<sub>2</sub>] was put into the balance pan, the reaction cell was closed, and a nitrogen flow of 20 cm<sup>3</sup>/min was maintained through the cell. Then a flow of reaction gas (methane, ethane, or propane) was directed over the sample instead of nitrogen. There was a very sharp mass increase after several seconds, the time necessary for gas to reach the sample. Then there was a further increase as all of the nitrogen in the reaction cell was replaced. To deliver

the reacting gas at a pressure close to 1 atm, the purge gas system outlet was equipped with a capillary. The experiment was continued until the sample weight became constant in time (typically 3 h).

*Method B* (Scheme 1, reaction 2) was quite similar to A, but  $\alpha$ -[CuL<sub>2</sub>] was used instead. Reactions required significantly more time, 1–3 days. There was a typical sigmoidal-shaped mass increase with time, and the final product was shown to be  $\beta$ -phase free of  $\alpha$ -form by X-ray powder diffraction. *n*-Butane and neopentane were used as reaction gases. To prepare a gas mixture with a partial pressure of isopentane, nitrogen was bubbled through a thermostated (20 °C) vessel filled with neat liquid.

In *Method C* (Scheme 1, reaction 2) samples of 100–150 mg of  $\alpha$ -[CuL<sub>2</sub>], or up to 400 mg for highly volatile guests, were used. These were placed in closed vessels along with saturated solutions of the host complex in the corresponding guest liquid (to create a guest vapor pressure which is equal to the equilibrium guest pressure over the inclusion with maximum guest content). For paraffins, pure guest liquids rather than their saturated solutions were used, as no difference was observed due to low solubility of the title complex in paraffins. Details of this method were given before.<sup>6</sup> For higher paraffins and alcohols, reactions were too slow and therefore higher temperatures were used. In all cases the final product was the  $\beta$ -phase.

Two independent determinations were made. Compositions  $x$  of the resulting  $\beta$ -[CuL<sub>2</sub>] $\cdot$  $x$ G clathrates were calculated from the formula  $x = (\Delta m/m_0)(M_H/M_G)$ , where  $\Delta m$  and  $m_0$  are the mass increase and the starting sample mass, and  $M_H$  and  $M_G$  are host and guest molecular masses, respectively. Method type, experimental temperatures, and results are given in Tables 1 and 3.

**Melting temperatures** and the type of melting process were determined visually. Samples prepared in the course of isopiestic experiments were sealed in capillary tubes with minimal free volume. The heating rate close to the melting point did not exceed 1°/min. The product liquor was always green, while the solid (from incongruent processes) was blue. Two or three determinations were made in less certain cases.

**Wetting Probe.** The host complex in its pure  $\alpha$ -form was wetted with the appropriate guest substance and the X-ray powder pattern of the wet or dry product was recorded immediately. If no phase change was observed, or if the change was incomplete, one or more of the following procedures was followed: grinding of the mixture, holding it for 1 or 2 h, or adding a little mesitylene. Product identification was performed by comparison of the X-ray diffraction pattern with those of the highly characteristic  $\alpha$ - and  $\beta$ -form patterns.<sup>6</sup> According to our experiences, formation of a green product without a phase change to either  $\alpha$ - or  $\beta$ -forms meant that ligation of the second component to the [CuL<sub>2</sub>] unit had taken place.<sup>37</sup>

**Single-Crystal Diffraction Analysis.** Single crystals of the compounds studied were taken from their mother liquors and immediately cooled to –100 °C at which temperature all further experiments were done. Data were collected using the  $\omega$  scan mode on a Siemens SMART CCD diffractometer with Mo  $K\alpha$  radiation

(35) The HL diketone is prepared in four steps. For earlier communications on the separate steps, see: (a) Merz, A. *Angew. Chem., Int. Ed. Engl.* **1973**, *12*, 846–847. (b) Sokolov, I. E.; Kotlyarevskii, I. L. *Izv. Akad. Nauk SSSR, Ser. Khim.* **1980**, 202–203 (in Russian); *Chem. Abstr.* **1980**, *92*, 214840x. (c) Shergina, S. I.; Sokolov, I. E.; Zanina, A. S. *Izv. Akad. Nauk SSSR, Ser. Khim.* **1992**, 158–160 (in Russian); *Chem. Abstr.* **1992**, *116*, 255138g. (d) Sokolov, I. E.; Shergina, S. I.; Zanina, A. S. *Izv. Akad. Nauk SSSR, Ser. Khim.* **1992**, 1390–1392 (in Russian); *Chem. Abstr.* **1993**, *118*, 124090d.

(36) See, for example, refs 5k and 7c, and also: Angla, B. *Ann. Chim.* **1949**, *4*, 639–698; *Chem. Abstr.* **1950**, *44*, 3442c.

**Table 5. Binary Products of Solvent Addition to  $\alpha$ -[CuL<sub>2</sub>]: Essential Properties, Parameters for the X-ray Experiments and Crystal Data**

solvent	<i>n</i> -hexane	<i>tert</i> -butanol	methanol	ethanol
resulting compound	$\beta$ -[CuL <sub>2</sub> ] $\cdot$ <i>x</i> ( <i>n</i> -hexane)	$\beta$ -[CuL <sub>2</sub> ] $\cdot$ <i>x</i> ( <i>tert</i> -butanol)	[Cu(MeOH) <sub>2</sub> L <sub>2</sub> ]	{[Cu(EtOH)L <sub>2</sub> ] <sub>2</sub> [CuL <sub>2</sub> ]}
moles of added solvent:				
from isopiestic experiment	<i>x</i> = 0.373(4)	<i>x</i> = 0.676(5)	<i>x</i> = 2.04(2)	<i>x</i> = 0.669(5)
from X-ray crystallography	<i>x</i> = 0.38(2)	<i>x</i> = <sup>2</sup> / <sub>3</sub>	<i>x</i> = 2	<i>x</i> = <sup>2</sup> / <sub>3</sub>
color:	blue	blue	green	bluish-green
stability in air	stable	stable	decomposes	decomposes
high limit of stability	147 °C, true melting	135.5 °C, incongruent melting	67 °C, incongruent melting	70 °C, incongruent melting
complex framework topology	3-D coordination polymer	3-D coordination polymer	2-D hydrogen-bond polymer	1-D coordination polymer
configuration of [CuL <sub>2</sub> ] unit	square-planar, <i>trans</i>	square-planar, <i>trans</i>	square-planar, <i>trans</i>	square-planar, 2 <i>cis</i> + 1 <i>trans</i>
formula/formula weight	C <sub>18.3</sub> H <sub>25.3</sub> CuF <sub>6</sub> O <sub>6</sub> /518.2	C <sub>18.7</sub> H <sub>26.7</sub> CuF <sub>6</sub> O <sub>6.7</sub> /535.3	C <sub>18</sub> H <sub>28</sub> CuF <sub>6</sub> O <sub>8</sub> /549.9	C <sub>52</sub> H <sub>72</sub> Cu <sub>3</sub> F <sub>18</sub> O <sub>20</sub> /1549.7
crystal system/space group	trigonal, <i>R</i> $\bar{3}$ (N 148)	trigonal, <i>R</i> $\bar{3}$ (N 148)	monoclinic, <i>P</i> <sub>2</sub> <sub>1</sub> / <i>c</i> (N 14)	monoclinic, <i>C</i> <sub>2</sub> / <i>c</i> (N 15)
unit cell dimensions (-100 °C)	<i>a</i> = 24.144(3) Å <i>c</i> = 10.434(2) Å <i>V</i> = 5267(1) Å <sup>3</sup> <i>Z</i> = 9	<i>a</i> = 24.221(4) Å <i>c</i> = 10.558(2) Å <i>V</i> = 5364(2) Å <sup>3</sup> <i>Z</i> = 9	<i>a</i> = 7.283(1) Å <i>b</i> = 9.710(1) Å <i>c</i> = 16.678(2) Å $\beta$ = 93.87(1)° <i>V</i> = 1176.7(2) Å <sup>3</sup> <i>Z</i> = 2	<i>a</i> = 35.695(4) Å <i>b</i> = 10.972(2) Å <i>c</i> = 19.793(3) Å $\beta$ = 117.73(1)° <i>V</i> = 6862(2) Å <sup>3</sup> <i>Z</i> = 4
calculated density	1.470 g cm <sup>-3</sup>	1.491 g cm <sup>-3</sup>	1.552 g cm <sup>-3</sup>	1.500 g cm <sup>-3</sup>
total/unique/intense <sup>a</sup> data	20430/3030/2783	20877/3099/2604	13119/3043/2763	40105/8896/7004
refined parameters	230	256	193	613
final <i>R</i> -values (intense data)	<i>R</i> = 0.037; <i>R</i> w <sup>2</sup> = 0.099	<i>R</i> = 0.052; <i>R</i> w <sup>2</sup> = 0.121	<i>R</i> = 0.038; <i>R</i> w <sup>2</sup> = 0.102	<i>R</i> = 0.032; <i>R</i> w <sup>2</sup> = 0.084
goodness of fit on <i>F</i> <sup>2</sup>	1.062	1.075	1.020	1.047
residual extrema	+0.50, -0.41 e Å <sup>-1</sup>	+0.61, -0.30 e Å <sup>-1</sup>	+0.70, -0.29 e Å <sup>-1</sup>	+0.42, -0.29 e Å <sup>-1</sup>

<sup>a</sup> Data with *I* > 2 $\sigma$ (*I*).

( $\lambda = 0.7107$  Å) and a graphite monochromator. Unit cell parameters were measured using all collected data. Absorption corrections were made using the SADABS routine. Solution and refinement were performed using direct methods (SHELXS-86) and full-matrix least-squares on *F*<sup>2</sup> (SHELXL-93) using all positive data.<sup>38</sup> Non-hydrogen atoms were refined anisotropically except for the guest atoms of the *n*-hexane inclusion. Hydrogen atoms were refined isotropically with thermal factors 1.2 times those of adjacent carbon atoms. Guest hydrogens were placed in calculated positions.

For the hexane inclusion, the host structure was determined first while a large number of maxima inside the channel space indicated strong disorder of the guest. About two-dozen guest molecules in different conformations were superimposed onto the available centers. Bond lengths and valence angles for the guest were fixed at known values while position, conformation, and occupation were allowed to change. During refinement the orientations with low or negative occupancy were removed successively until two remained.

For all structures, residual maxima on the electron density map were located near copper atoms. Selected experimental details, crystal data and relevant properties of compounds studied are listed in Table 5.

**Powder Diffraction Measurements** were performed on a Rigaku Geigerflex diffractometer, Co K $\alpha$  radiation ( $\lambda = 1.7902$  Å). Powder patterns of four

crystalline samples studied by single-crystal X-ray diffraction were found to correspond well to powder patterns of the same compounds prepared in the course of the isopiestic experiments.

**Analysis of Packing.** Channel space profiles were calculated on the basis of the crystallographic data with the CLAT software package<sup>39</sup> and the Zefirov-Zorkii system of van der Waals radii (C, 1.71; H, 1.16; Cu, 1.40; F, 1.35; O, 1.29 Å).<sup>40</sup>

**Acknowledgment.** This work was supported by a Visiting Fellowship for D.V.S. We thank researchers at the Steacie Institute for Molecular Sciences for assistance, especially Drs. K. A. Udachin and G. D. Enright for consultation on the crystallographic studies, Dr. C. I. Ratcliffe for helpful suggestions, Drs. S. Lang and S. Breeze for consultations on the preparation of this manuscript. We also thank Dr. A. B. Burdukov (International Tomography Center, Novosibirsk) and D. A. Gushchin (Institute of Inorganic Chemistry, Novosibirsk) for providing relevant literature, and E. V. Grachev (ICh, Novosibirsk) for making the CLAT software package available.

**Supporting Information Available:** Full tables of crystal data and structural refinements, bond lengths and angles, anisotropic displacement parameters, and hydrogen atom parameters for  $\beta$ -[CuL<sub>2</sub>] $\cdot$ *x*(*n*-hexane),  $\beta$ -[CuL<sub>2</sub>] $\cdot$ *x*(*tert*-butanol), [Cu(MeOH)<sub>2</sub>L<sub>2</sub>] and {[Cu(EtOH)L<sub>2</sub>]<sub>2</sub>[CuL<sub>2</sub>]}. This material is available free of charge via the Internet at <http://pubs.acs.org>.

CM990759D

(37) It should be noted that solutions of [CuL<sub>2</sub>] are colored blue if the solvent does not contain donor atoms, and green for solvents capable of coordinating to the metal centers (alcohols, ethers, nitriles, etc.).

(38) (a) Sheldrick, G. M. *Acta Crystallogr.* **1990**, *A46*, 467–473. (b) Sheldrick, G. M. *Acta Crystallogr.* **1993**, *A49*, C53.

(39) Grachev, E. V.; Dyadin, Yu. A.; Lipkowski, J. *J. Struct. Chem.* **1995**, *36*, 876–879.

(40) Zefirov, Yu. V.; Zorkii, P. M. *Russ. Chem. Rev.* **1995**, *64*, 415–428.